

Joint Optimization of DNN Inference Delay and Energy under Accuracy Constraints for AR Applications

Guangjin Pan[†], Heng Zhang[†], Shugong Xu[†], Shunqing Zhang[†], and Xiaojing Chen[†]

[†] Key laboratory of Specialty Fiber Optics and Optical Access Networks,
Shanghai University, Shanghai, 200444, China

Email: {guangjin_pan, hengzhang, shugong, shunqing, jodiechen}@shu.edu.cn

Abstract—The high computational complexity and high energy consumption of artificial intelligence (AI) algorithms hinder their application in augmented reality (AR) systems. This paper considers the scene of completing video-based AI inference tasks in the mobile edge computing (MEC) system. We use multiply-and-accumulate operations (MACs) for problem analysis and optimize delay and energy consumption under accuracy constraints. To solve this problem, we first assume that offloading policy is known and decouple the problem into two subproblems. After solving these two subproblems, we propose an iterative-based scheduling algorithm to obtain the optimal offloading policy. We also experimentally discuss the relationship between delay, energy consumption, and inference accuracy.

Index Terms—Mobile augmented reality, edge intelligence, mobile edge computing, resource allocation.

I. INTRODUCTION

The metaverse requires people to interact between the real world and the virtual world. Augmented reality (AR) is an essential technology for this to happen. With artificial intelligence (AI) technology, AR can carry out more profound scene understanding and more immersive interactions.

AI has played an essential role in many fields, such as automatic speech recognition (ASR), natural language processing (NLP), computer vision (CV), and so on. However, the computational complexity of AI algorithms, especially deep neural networks (DNN), is usually very high. It is challenging to complete DNN inference timely and reliably on mobile devices with limited computation and energy capacity. In [1], experiments show that a typical single-frame image processing AI inference task takes about 600 ms even with speedup from the mobile GPU. In addition, continuously executing the above inference tasks can only last up to 2.5 hours on commodity devices. The above issues result in only a few AR applications currently using deep learning. To reduce the inference time of DNNs, one way is to perform network pruning on the neural network [2]–[4]. However, it could be destructive to the model if pruning too many channels, and it may not be possible to recover a satisfactory accuracy by fine-tuning [2].

Edge AI [5]–[7] is another approach to solving these problems. The integration of mobile edge computing (MEC) and AI technology has recently become a promising paradigm for supporting computationally intensive tasks. The edge DNN

inference tasks need to consider three Key Performance Indicators (KPIs), i.e., delay, energy consumption, and accuracy. [8] and [9] optimize inference task selection to minimize the energy consumption in wireless networks. To optimize the inference delay, [10] uses a tandem queueing model to analyze the queueing and processing delays of DL tasks in multiple DNN partitions. At the same time, [11] and [12] optimize the accuracy of inference tasks under the constraints of delay and energy consumption. What's more, [13] joint optimizes the service placement, computational and radio resource allocation to minimize the users' total delay and energy consumption.

In this paper, we consider a multi-user MEC system and assume that each device executes the video-based DNN inference task. Each device can be AR glasses, mobile robots, and so on. Different from the offloading problem of still-based (image-based or single-frame-video-based) DNN inference tasks in existing studies [10]–[12], we focus on the video-based DNN inference tasks, which have higher computational complexity and require more computing energy. We model the problem as a multi-objective optimization problem to optimize delay and energy consumption with the constraint of inference accuracy. The main contributions of this paper are summarized as follows,

- *Multi-dimensional target optimization.* We formulate the video-based offloading problem as a mixed-integer non-linear programming problem (MINLP). Unlike existing work [13], we optimize latency and energy consumption under the constraints of DNN inference accuracy. To the best of our knowledge, this is the first work that considers the relationship between delay, energy, and accuracy at the same time. At the same time, we also explore the trade-off relationship between latency, energy consumption and inference accuracy.
- *MAC-based analysis model.* We explored the relationship between the number of input video frames and delay, energy consumption and inference accuracy. We also use multiply-and-accumulate operations (MACs) for refined modeling for the delay and energy consumption. To our knowledge, this is the first work using MACs to analyze the AI inference offloading problem.

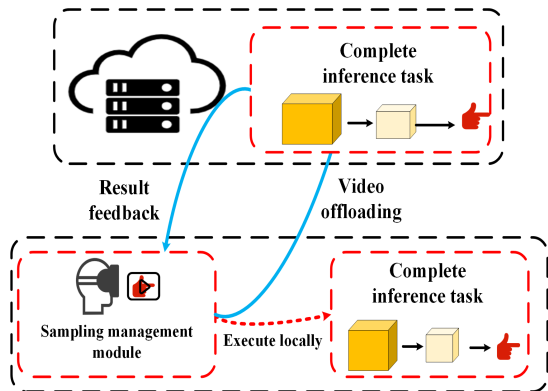


Fig. 1. The overview of the video sampling and computing offloading system. The video sampling management module can control the sampling rate of the captured video and determine the number of video frames used for AI inference. Devices can transmit the video to the edge server or perform inference tasks locally based on the wireless channel information and computing capabilities.

- *Iteration-based scheduling scheme.* To solve the optimization problem, we decompose the original problem. First, assuming that the offloading decision is given, we respectively solve optimization problems of the device set that completes the inference locally and the device set that is offloaded to the edge server. Then, to obtain the optimal offloading policy, we propose a iterative-based algorithm and solve the original problem through iteration.

The rest of this paper is organized as follows. In Section II, we introduce system models, including delay, energy, and accuracy models. In Section III, we formulate the joint optimization problem and convert the original problem to make it more tractable. Section IV gives the solution algorithm of the proposed problem. Numerical results and analysis are presented in Section V. Finally, the paper is concluded in Section VI.

II. SYSTEM MODEL

We consider a multi-user MEC system with one base station (BS) and N mobile devices, denoted by the set $\mathcal{N} = \{1, 2, \dots, N\}$. Each device has a camera and needs to accomplish DNN inference tasks. Due to the limitation of device computational resources, DNN inference tasks can be placed on local or edge servers. The limited computational resource will lead to longer computing delay and greater power consumption when the inference task is executed locally. However, when the inference task is executed on the edge server, it will bring additional wireless transmission delay.

A. Delay and Energy Models for Inference

The inference delay depends on the DNN model's architecture, the input size of the DNN model, and the device's or server's computing power. The computational complexity of the n^{th} device's task can be expressed as $C(M_n, d_n, \Theta_n)$, where M_n is the number of input video frames, d_n is the data size of one video frame, and Θ_n represents the architecture and parameters of the DNN. In this paper, we mainly focus on the

impact of the number of input video frames M_n on recognition accuracy and the allocation of communication and computing resources. We assume that both d_n and Θ_n are same for different devices. Therefore, we simplify the expression of the computational complexity to $C(M_n)$. $C(M_n)$ also means the number of MACs that DNN inference needs to complete, when the number of input video frames is M_n .

Then we give the expression for the inference delay and energy consumption. The computation delay of the device n and MEC can be respectively expressed as,

$$D_n^{md} = \frac{\rho C(M_n)}{f_n^{md}}, \quad (1)$$

$$D_n^e = \frac{\rho C(M_n)}{f_n^e}, \quad (2)$$

where ρ (cycle/MAC) represents the number of CPU cycles required to complete a multiplication and addition, which depends on the CPU model. f_n^e and f_n^{md} (in CPU cycle/s) represent the computing resources allocated by the edge server and the device, respectively. Denote $f_n^{e,max}$ and $f_n^{md,max}$ to be the total computation resource of the edge server and the mobile device n , respectively. Therefore, the computing resources satisfy $\sum_{n \in \mathcal{N}} f_n^e \leq f_n^{e,max}$ and $f_n^{md} \leq f_n^{md,max}$.

As for energy consumption, denote κ to be a coefficient determined by the corresponding device [11]. The computational energy consumption of device n can be expressed as,

$$E_n^{md} = \kappa \rho C(M_n) f_n^{md^2}. \quad (3)$$

B. Delay and Energy Models for Transmission

We consider a time-division multiple access (TDMA) method for channel access. Denote R_n to be the achievable data rate of device n . The delay and energy consumption of transmission can be written as,

$$D_n^t = \frac{M_n d_n}{R_n t_n}, \quad (4)$$

$$E_n^t = \frac{M_n d_n}{R_n} p_n. \quad (5)$$

where t_n is the proportion of time that device n transmits, and p_n is the transmission power.

C. Inference Tasks Accuracy Model

As mentioned above, we mainly focus on the impact of the number of input video frames M_n on recognition accuracy. We assume that the quality of the input video is the same for different devices. For a certain task and DNN model, the accuracy is only determined by the number of input frames. According to [14], more frames will lead to better inference accuracy, and as the input frames continue to increase, the performance gain will gradually decrease. Take gesture and action recognition as examples. Fig. 2 shows the relationship between the inference accuracy and the number of input video frames. Therefore, we define $\Phi(M_n)$ as a monotone non-decreasing function to describe the relationship between the accuracy and the number of input frames.

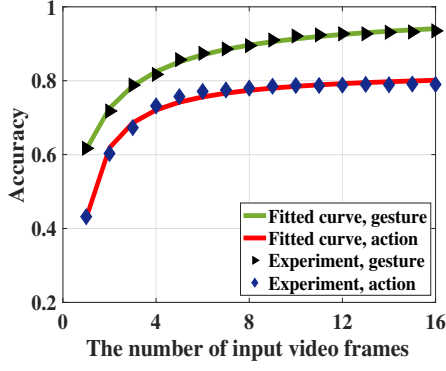


Fig. 2. The experimental and fitted curves of gesture recognition task and action recognition task.

III. PROBLEM FORMULATION

In this section, we formulate the optimization problem to reduce the system's delay and devices' energy consumption under the constraint of recognition accuracy. We analyze the difficulty of solving the problem. To simplify the problem, we make a reasonable conversion of the problem.

A. Original Problem Formulation

Based on the above analysis, the n^{th} device's delay and energy consumption can be expressed as,

$$D_n = (1 - x_n) \frac{\rho C(M_n)}{f_n^{md}} + x_n \left(\frac{\rho C(M_n)}{f_n^e} + \frac{M_n d_n}{R_n t_n} \right), \quad (6)$$

$$E_n = (1 - x_n) \kappa \rho C(M_n) f_n^{md2} + x_n \left(\frac{M_n d_n}{R_n} p_n \right). \quad (7)$$

where x_n indicates whether the inference task is executed on local or edge servers.

Given the system model described previously, our goal is to reduce end-to-end delay and energy consumption under the constraint of recognition accuracy. Each device follows the binary offloading policy. The mathematical optimization problem of the total cost can be expressed as,

Problem $\mathcal{P}1$ (Original Problem):

$$\underset{\{M_n, t_n, f_n^{md}, f_n^e, x_n\}}{\text{minimize}} \quad \sum_{n \in \mathcal{N}} \left(\beta_1 D_n + \beta_2 E_n \right), \quad (8)$$

$$\text{subject to} \quad \Phi(M_n) \geq \alpha_n, \quad \forall n \in \mathcal{N}, \quad (8a)$$

$$M_n \leq M_n^{max}, \quad M_n \in \mathbb{Z}, \quad (8b)$$

$$\sum_{n \in \mathcal{N}} x_n t_n \leq 1, \quad (8c)$$

$$\sum_{n \in \mathcal{N}} x_n f_n^e \leq f_n^{e,max}, \quad (8d)$$

$$t_n, f_n^e \geq 0, \quad \forall n \in \mathcal{N}, \quad (8e)$$

$$0 \leq f_n^{md} \leq f_n^{md,max}, \quad \forall n \in \mathcal{N}, \quad (8f)$$

$$x_n \in \{0, 1\}, \quad \forall n \in \mathcal{N}, \quad (8g)$$

where α_n represents the recognition accuracy requirement, β_1, β_2 are the weight factors. (8a) represents the recognition accuracy requirement of each device. (8b) indicates the frame

limit for the input video, \mathbb{Z} is the set of integers, and M_n^{max} is the maximum number of frames of the input video. (8c) and (8d) represent the communication and computation resource limitation, respectively. (8f) limits the computation resource of each device.

Problem $\mathcal{P}1$ is a non-convex MINLP problem and is difficult to be solved. First, $C(M_n)$ is a discrete function. As the number of input frames M_n increases, the computational complexity also increases. This kind of increase is irregular because it is affected by the structure of DNN layers, such as the stride and padding size of 3DCNN. Therefore, $C(M_n)$ cannot be used for optimization directly. Second, both M_n and x_n are integers, making the problem difficult to be solved.

B. Problem Conversion

To make the problem $\mathcal{P}1$ more tractable, we convert the problem. First, we give an approximate expression of the computational complexity function $C(M_n)$, and assume it is a continuous function.

Second, considering that $\Phi(M_n)$ is a monotone non-decreasing function. In order not to lose generality, define $M_n^* = \arg \min_{M_n} \Phi(M_n)$, $\Phi(M_n) \geq \alpha_n$, $M_n \in \mathbb{Z}$. M_n^* is the minimum number of input frames under the requirement of accuracy.

We define two sets of devices, i.e. $\mathcal{N}_0 = \{n \mid x_n = 0, n \in \mathcal{N}\}$ and $\mathcal{N}_1 = \{n \mid x_n = 1, n \in \mathcal{N}\}$. $\mathcal{F}_{0,n}$ and $\mathcal{F}_{1,n}$ are the cost function of the device n in sets \mathcal{N}_0 and \mathcal{N}_1 , respectively. As mentioned above, the problem $\mathcal{P}1$ can be rewritten as,

Problem $\mathcal{P}2$ (Converted Problem):

$$\underset{\{t_n, f_n^{md}, f_n^e, x_n\}}{\text{minimize}} \quad \sum_{n \in \mathcal{N}_0} (1 - x_n) \mathcal{F}_{0,n}(M_n^*, f_n^{md}) + \sum_{n \in \mathcal{N}_1} x_n \mathcal{F}_{1,n}(M_n^*, f_n^e, t_n), \quad (9)$$

subject to (8c) – (8g),

where

$$\mathcal{F}_{0,n}(M_n^*, f_n^{md}) = \beta_1 \frac{\rho C(M_n^*)}{f_n^{md}} + \beta_2 \kappa \rho C(M_n^*) f_n^{md2}, \quad (10)$$

$$\mathcal{F}_{1,n}(M_n^*, f_n^e, t_n) = \beta_1 \frac{\rho C(M_n^*)}{f_n^e} + \beta_1 \frac{M_n^* d_n}{R_n t_n} + \beta_2 \frac{M_n^* d_n p_n}{R_n}. \quad (11)$$

IV. OPTIMIZATION PROBLEM SOLVING

In this section, we decompose the problem $\mathcal{P}2$ and propose a iterative-based greedy scheme to solve it. First, supposing that the offloading decision (i.e. $\{x_n\}$) is given, we solve optimization problems of sets \mathcal{N}_0 and \mathcal{N}_1 , respectively. Then, we propose a iterative-based algorithm to optimize the offloading decision $\{x_n\}$.

A. Optimization Problem Solving for \mathcal{N}_0

For set \mathcal{N}_0 , i.e., when the device executes inference tasks locally, the optimization problem becomes,

Problem $\mathcal{P}_{\mathcal{N}_0}$ (Problem for \mathcal{N}_0):

$$\underset{\{f_n^{md}\}}{\text{minimize}} \quad \mathcal{F}_{\mathcal{P}_{\mathcal{N}_0}} \triangleq \sum_{n \in \mathcal{N}_0} \mathcal{F}_{0,n}(M_n^*, f_n^{md}), \quad (12)$$

subject to (8f).

The optimization variables in $\mathcal{P}_{\mathcal{N}_0}$ is the local computation resource f_n^{md} . We can derive the optimal solution to $\mathcal{P}_{\mathcal{N}_0}$ in a closed-form expression.

Theorem 1: The optimal solution to $\mathcal{P}_{\mathcal{N}_0}$ is given by,

$$f_n^{md*} = \min\left\{\sqrt[3]{\left(\frac{\beta_1}{2\beta_2\kappa}\right)}, f_n^{md,max}\right\} \quad (13)$$

Proof: Please refer to Appendix A.

The partial derivative of $\mathcal{F}_{\mathcal{P}_{\mathcal{N}_0}}$ with respect to f_n^{md} is,

$$\frac{\partial \mathcal{F}_{\mathcal{P}_{\mathcal{N}_0}}}{\partial f_n^{md}} = -\beta_1 \frac{\rho C(M_n^*)}{f_n^{md2}} + 2\beta_2\kappa\rho C(M_n^*)f_n^{md}, \quad (14)$$

By setting $\frac{\partial \mathcal{F}_{\mathcal{P}_{\mathcal{N}_0}}}{\partial f_n^{md}} = 0$, we have,

$$f_n^{md} = \sqrt[3]{\left(\frac{\beta_1}{2\beta_2\kappa}\right)}. \quad (15)$$

Considering the value range of f_n^{md} , the optimal solution can be given by,

$$f_n^{md*} = \min\left\{\sqrt[3]{\left(\frac{\beta_1}{2\beta_2\kappa}\right)}, f_n^{md,max}\right\} \quad (16)$$

which completes the proof.

From *Theorem 1*, we can see that the optimal local CPU-cycle frequency f_n^{md} is determined by the weight factors β_1 , β_2 , the coefficient of CPU energy consumption κ , and is limited by its corresponding upper bound $f_n^{md,max}$.

B. Optimization Problem Solving for \mathcal{N}_1

Then we solve the optimization problem of \mathcal{N}_1 . The problem \mathcal{P}_2 can be written as,

Problem $\mathcal{P}_{\mathcal{N}_1}$ (Problem for \mathcal{N}_1):

$$\underset{\{f_n^e, t_n\}}{\text{minimize}} \quad \sum_{n \in \mathcal{N}_1} \mathcal{F}_{1,n}(M_n^*, f_n^e, t_n), \quad (17)$$

subject to (8c), (8d), (8e).

The optimization variables in the the problem $\mathcal{P}_{\mathcal{N}_1}$ are the edge computation resource f_n^e , and the proportion of transmission time t_n . We can obtain the optimal solution to $\mathcal{P}_{\mathcal{N}_1}$ using the method of Lagrange multiplier. The partial Lagrangian function can be written as,

$$\begin{aligned} \mathcal{L}_{\mathcal{P}_{\mathcal{N}_1}} = & \sum_{n \in \mathcal{N}_1} \left(\frac{\beta_1 \rho C(M_n^*)}{f_n^e} + \frac{\beta_1 M_n^* d_n}{R_n t_n} + \frac{\beta_2 M_n^* d_n p_n}{R_n} \right) \\ & + \mu_0 \left(\sum_{n \in \mathcal{N}_1} t_n - 1 \right) + \mu_1 \left(\sum_{n \in \mathcal{N}_1} f_n^e - f_n^{e,max} \right), \quad (18) \end{aligned}$$

First of all, according to (18), supposing that M_n^* is given, we can solve the problem $\mathcal{P}_{\mathcal{N}_1}$ based on the Karush-Kuhn-Tucker (KKT) condition. We can obtain the function expressions of f_n^{e*} and t_n^* relative to M_n^* , as shown in the following theorem.

Theorem 2: The function expressions of f_n^{e*} and t_n^* relative to M_n^* are given by,

$$f_n^{e*} = \frac{f_n^{e,max} \sqrt{C(M_n^*)}}{\sum_{i \in \mathcal{N}_1} \sqrt{C(M_i^*)}}, \quad (19)$$

$$t_n^* = \frac{\sqrt{\frac{M_n^*}{R_n}}}{\sum_{i \in \mathcal{N}_1} \sqrt{\frac{M_i^*}{R_i}}}. \quad (20)$$

Proof: Please refer to Appendix B.

According to the KKT conditions, we can obtain the following necessary and sufficient conditions,

$$\frac{\partial \mathcal{L}_{\mathcal{P}_{\mathcal{N}_1}}}{\partial f_n^{e*}} = -\frac{\beta_1 \rho C(M_n^*)}{f_n^{e*2}} + u_1^* = 0, \quad f_n^{e*} > 0, \quad (21)$$

$$\frac{\partial \mathcal{L}_{\mathcal{P}_{\mathcal{N}_1}}}{\partial t_n^*} = -\frac{\beta_1 M_n^* d_n}{R_n t_n^{*2}} + u_0^* = 0, \quad t_n^* > 0, \quad (22)$$

$$\mu_0^* \left(\sum_{n \in \mathcal{N}^*} t_n^* - 1 \right) = 0, \quad (23)$$

$$\mu_1^* \left(\sum_{n \in \mathcal{N}^*} f_n^{e*} - f_n^{e,max} \right) = 0, \quad (24)$$

$$\mu_0^*, \mu_1^* \geq 0. \quad (25)$$

Because $\frac{\beta_1 \rho C(M_n^*)}{f_n^{e*2}}$ and $\frac{\beta_1 M_n^* d_n}{R_n t_n^{*2}}$ are both positive, μ_0^* and μ_1^* are also positive. Therefore, we can obtain,

$$\sum_{n \in \mathcal{N}} f_n^{e*} - f_n^{e,max} = 0, \quad (26)$$

$$\sum_{n \in \mathcal{N}} t_n^* - 1 = 0, \quad (27)$$

$$f_n^{e*} = \sqrt{\frac{\beta_1 \rho C(M_n^*)}{R_n \mu_1^*}}, \quad (28)$$

$$t_n^* = \sqrt{\frac{\beta_1 M_n^* d_n}{R_n \mu_0^*}}. \quad (29)$$

Combining (26) and (28), we can get the expression of f_n^{e*} corresponding to M_n^* ,

$$f_n^{e*} = \frac{f_n^{e,max} \sqrt{C(M_n^*)}}{\sum_{i \in \mathcal{N}_1} \sqrt{C(M_i^*)}}. \quad (30)$$

Similarly, combining (27) and (29), we can get the expression of t_n^* corresponding to M_n^* ,

$$t_n^* = \frac{\sqrt{\frac{M_n^*}{R_n}}}{\sum_{i \in \mathcal{N}_1} \sqrt{\frac{M_i^*}{R_i}}}. \quad (31)$$

which completes the proof.

C. Optimization of Offloading Policy $\{x_n\}$

We can use the Enumeration method to search for all offloading strategies and get the optimal solution. However, the complexity of Search-based offloading decision algorithm becomes high when the number of devices N grows large.

In this section, we propose an iterative-based greedy algorithm to optimize the offloading decision $\{x_n\}$. Then, we analyze the computational complexity of our proposed algorithms. Inspired by the *Theorem 1* and *Theorem 2*, when executing inference locally, the cost function $\mathcal{F}_{0,n}$ and optimization variables f_n^{md} , M_n only depend on the device's own parameters and are not affected by the parameters of other devices. However, for edge set \mathcal{N}_1 , the cost function is related to the number and parameters of devices in the set \mathcal{N}_1 . The principle of the iterative-based algorithm is introduced as follows. First, calculate the cost function $\{\mathcal{F}_{0,n}\}$ of set \mathcal{N}_0 when each device's task is executed locally. Second, assuming that all devices are offloaded to the edge server for inference and $|\mathcal{N}_1| = N$. In each iteration, the cost function $\{\mathcal{F}_{1,n}\}$ corresponding to each device of \mathcal{N}_1 is obtained. Comparing $\{\mathcal{F}_{0,n}\}$ and $\{\mathcal{F}_{1,n}\}$ of the devices in the \mathcal{N}_1 set, we can get the difference between $\{\mathcal{F}_{0,n}\}$ and $\{\mathcal{F}_{1,n}\}$ and select the device with the largest difference as k . Try to put the device k from the set \mathcal{N}_1 into the set \mathcal{N}_0 and compute the cost of new sets. If the total cost of new sets is reduced, continue the next iteration. Otherwise, put the device k back to the set \mathcal{N}_1 .

V. NUMERICAL RESULTS

In this section, we evaluate the performance of the proposed algorithms via simulations. For all the simulation results, unless specified otherwise, we set the downlink bandwidth as $B_w = 5$ MHz and the power spectral as $N_0 = -174$ dBm/Hz [11]. According to [8], the path loss is modelled as $PL = 128.1 + 37.6 \log_{10}(D)$ dB, where D is the distance between the device and the BS in kilometres. Devices randomly distributed in the area within [500m 500m]. The computational resource of the MEC server and devices are set to be 1.8 GHz and 22 GHz, respectively. The recognition accuracy requirement and the maximum number of input video frames are set to $\alpha = 0.90$, $M_n^{max} = 16$, respectively. The coefficient κ is determined by the corresponding device and is set to be 10^{-28} in this paper according to [11]. The size of the input video is $112 * 112 * M_n$. In addition, the coefficient of computational complexity ρ is set to be 0.12 cycle/MAC, which is obtained through several experiments. Weights β_1 , β_2 are set to be 0.5, 0.5, respectively. The default number of users is 20. We perform experimental analysis with the gesture recognition task and the Resnet-18 network.

A. Simulation Results of Average Cost

In this section, we compare proposed algorithms and some baseline algorithms. We mainly compare the average cost. We run 100 tests and can calculate the average cost of each device and the average running time of each test.

In Fig. 3, we plot the average cost of the proposed scheme and some baseline schemes under a different number of devices. The proposed scheme is compared with the local inference scheme (Local), the edge inference scheme (Edge), and the random offloading scheme (Random). When the number of devices is less than 8, the cost of the scheme that executes tasks only at the edge is almost equal to the cost of

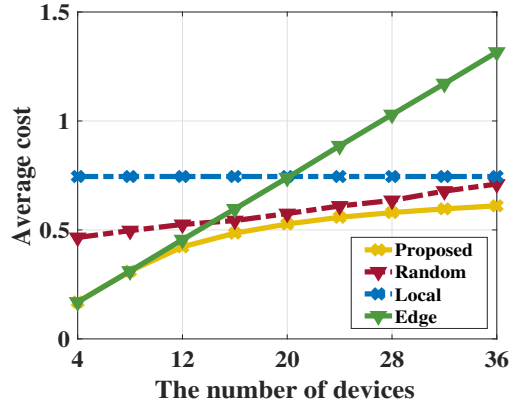


Fig. 3. Comparison of the proposed scheme and three baseline schemes. When there are only a small number of devices, the average cost of the proposed scheme and the scheme that devices are randomly offloaded to the edge server to complete inference tasks with 50% probability.

the proposed scheme. It is because all devices can benefit from performing inference on the edge server when the number of devices is small. If the inference task is only executed locally, the average cost of the device will not change because the local resources among the equipment do not affect each other. The curve for the Edge scheme is linear because we assume that the AI model is the same for all users.

B. Simulation Results of Delay, Energy, and Accuracy

This section compares the average delay, energy consumption, and the offloading rate (the proportion of devices that perform inference on the edge server). We set the default requirement for inference accuracy to be 0.9. We consider the different number of devices, different bandwidths, different edge computing resources, and different weights β_1 , β_2 .

Fig. 4 shows the average delay, energy, and offloading rate under different numbers of devices, different bandwidths, and different edge computing resources. In Fig. 4(a), we plot results with different numbers of devices. As shown in Fig. 4(a), when the number of devices is small (less than 8), with the number of devices increasing, the average delay increases, and the average energy consumption decrease. This is because when the number of devices is less than 8, all devices offload the task to the edge server (the offloading rate is equal to 1). With the number of devices increasing, communication resources and the edge server's computation resources are shared by more devices. It leads to an increase in the delay and a decrease in the number of input video frames for inference. When the number of devices exceeds 8, the average energy consumption increase, and the average delay and offload rate gradually decrease. Considering different bandwidths and different edge computing resources, we plot Fig. 4(b) and Fig. 4(c). As shown in Fig. 4(b) and Fig. 4(c), the offloading rate increases with the bandwidth and edge computing resource increasing, indicating that more devices are offloading tasks to the edge server.

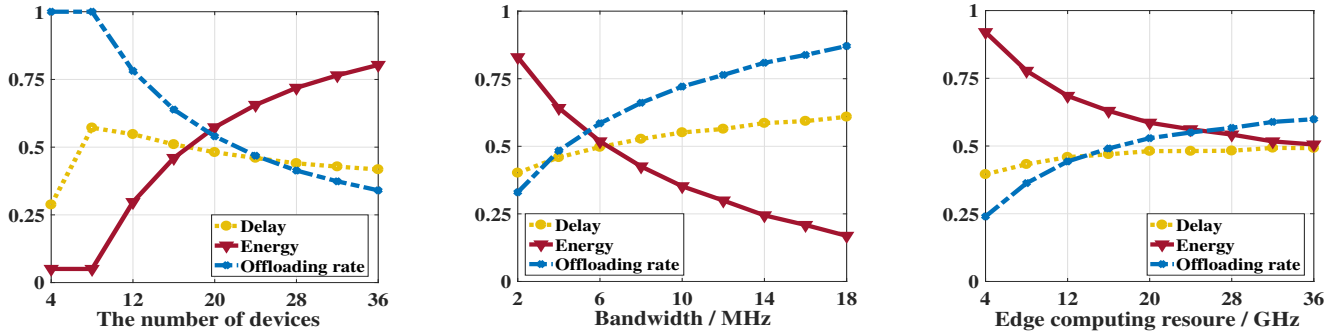


Fig. 4. The average delay, energy, and offloading rate under different numbers of devices, different bandwidths, and different edge computing resources.

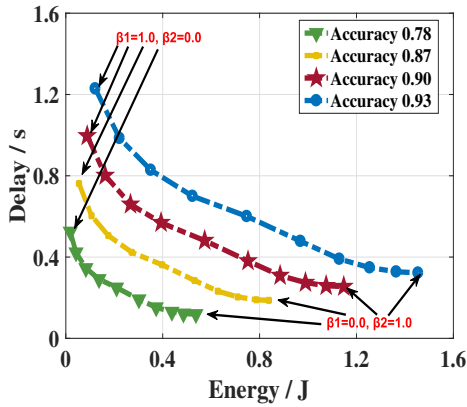


Fig. 5. The relationship between the delay, energy consumption, and accuracy.

We use different weights, β_1 , β_2 to study the trade-off relationship between the average delay and energy consumption with accuracy requirement. The constraint is $\beta_1 + \beta_2 = 1$. Fig. 5 shows the delay, energy consumption, and accuracy are mutually limited. Lower energy consumption leads to higher delay when the accuracy is constant. From another perspective, to improve the accuracy, it is necessary to sacrifice the performance of delay and energy consumption.

VI. CONCLUSION

This paper considers optimizing video-based AI inference tasks in a multi-user MEC system. An MINLP is formulated to minimize the total delay and energy consumption, with the requirement of accuracy. We use a MAC-based model to analyze the problem. We propose an iterative-based scheduling method to solve this problem. We analyze the experimental results with the different number of devices, different bandwidths and different edge computing capabilities. We also plot the relationship curve of the average delay, energy consumption, and accuracy.

ACKNOWLEDGEMENT

This work was supported in part by the National Natural Science Foundation of China (NSFC) under Grant 61871262, 62071284, and 61901251, the National Key R&D Program of China grants 2017YFE0121400 and 2019YFE0196600, the

Innovation Program of Shanghai Municipal Science and Technology Commission grants 20JC1416400 and 21ZR1422400, Pudong New Area Science & Technology Development Fund, Key-Area Research and Development Program of Guangdong Province grant 2020B0101130012, Foshan Science and Technology Innovation Team Project grant FS0AA-KJ919-4402-0060, and research funds from Shanghai Institute for Advanced Communication and Data Science (SICS).

REFERENCES

- [1] L. N. Huynh, R. K. Balan, and Y. Lee, "Deepsense: A gpu-based deep convolutional neural network framework on commodity mobile devices," in *Proc. ACM WearSys'16*, 2016, p. 25–30.
- [2] Z. Liu, J. Li, Z. Shen, G. Huang, S. Yan, and C. Zhang, "Learning efficient convolutional networks through network slimming," in *Proc. IEEE ICCV'17*, Oct 2017, pp. 2736–2744.
- [3] Z. Liu, M. Sun, T. Zhou, G. Huang, and T. Darrell, "Rethinking the value of network pruning," in *Proc. ICLR'19*, May 2019, pp. 1–21.
- [4] W. Shi, Y. Hou, S. Zhou, Z. Niu, Y. Zhang, and L. Geng, "Improving device-edge cooperative inference of deep learning via 2-step pruning," in *Proc. IEEE INFOCOM WKSHPs'19*, 2019, pp. 1–6.
- [5] Y. Shi, K. Yang, T. Jiang, J. Zhang, and K. B. Letaief, "Communication-efficient edge AI: Algorithms and systems," *IEEE Commun. Surveys Tuts.*, vol. 22, no. 4, pp. 2167–2191, 2020.
- [6] X. Wang, Y. Han, C. Wang, Q. Zhao, X. Chen, and M. Chen, "In-edge AI: Intelligentizing mobile edge computing, caching and communication by federated learning," *IEEE Netw.*, vol. 33, no. 5, pp. 156–165, 2019.
- [7] K. B. Letaief, Y. Shi, J. Lu, and J. Lu, "Edge artificial intelligence for 6G: Vision, enabling technologies, and applications," *IEEE J. Sel. Areas Commun.*, vol. 40, no. 1, pp. 5–36, 2022.
- [8] K. Yang, Y. Shi, W. Yu, and Z. Ding, "Energy-efficient processing and robust wireless cooperative transmission for edge inference," *IEEE Internet Things J.*, vol. 7, no. 10, pp. 9456–9470, 2020.
- [9] S. Hua, Y. Zhou, K. Yang, Y. Shi, and K. Wang, "Reconfigurable intelligent surface for green edge inference," *IEEE Transactions on Green Communications and Networking*, vol. 5, no. 2, pp. 964–979, 2021.
- [10] W. He, S. Guo, S. Guo, X. Qiu, and F. Qi, "Joint DNN partition deployment and resource allocation for delay-sensitive deep learning inference in IoT," *IEEE Internet Things J.*, vol. 7, no. 10, pp. 9241–9254, 2020.
- [11] Y. He, J. Ren, G. Yu, and Y. Cai, "Optimizing the learning performance in mobile augmented reality systems with CNN," *IEEE Trans. Wireless Commun.*, vol. 19, no. 8, pp. 5333–5344, 2020.
- [12] E. Li, L. Zeng, Z. Zhou, and X. Chen, "Edge AI: On-demand accelerating deep neural network inference via edge computing," *IEEE Trans. Wireless Commun.*, vol. 19, no. 1, pp. 447–457, 2020.
- [13] Z. Lin, S. Bi, and Y.-J. A. Zhang, "Optimizing AI service placement and resource allocation in mobile edge intelligence systems," *IEEE Trans. Wireless Commun.*, vol. 20, no. 11, pp. 7257–7271, 2021.
- [14] C. Wang, S. Zhang, Y. Chen, Z. Qian, J. Wu, and M. Xiao, "Joint configuration adaptation and bandwidth allocation for edge-based real-time video analytics," in *Proc. IEEE INFOCOM'20*, 2020, pp. 257–266.